



Loss of nitrogen via anaerobic ammonium oxidation (anammox) in the California Current system during the late Quaternary

Zoë Rebecca van Kemenade¹, Zeynep Erdem¹, Ellen Christine Hopmans¹, Jaap Smede Sinninghe Damsté^{1,2}, and Darci Rush¹

¹Department of Marine Microbiology and Biogeochemistry, Royal Netherlands Institute for Sea Research (NIOZ), P.O. Box 59, 1790 AB, Den Burg, the Netherlands

²Department of Earth Sciences, Utrecht University, Princetonlaan 8a, 3584 CB, Utrecht, the Netherlands

Correspondence: Zoë Rebecca van Kemenade (zoe.van.kemenade@nioz.nl)

Received: 4 December 2023 – Discussion started: 14 December 2023

Revised: 7 February 2024 – Accepted: 13 February 2024 – Published: 22 March 2024

Abstract. The California Current system (CCS) hosts one of the largest oxygen minimum zones (OMZs) in the world: the eastern North Pacific (ENP) OMZ, which is dissociated into subtropical and tropical regions (i.e. the ESTNP and ETNP). In the modern ENP OMZ, bioavailable nitrogen (N) is lost via denitrification and anaerobic ammonium oxidation (anammox). Even so, paleo-reconstructions of N loss have focused solely on denitrification. Fluctuations in bulk sedimentary $\delta^{15}\text{N}$ over glacial–interglacial cycles have been interpreted to reflect variations in denitrification rates in response to ETNP OMZ intensity changes. This $\delta^{15}\text{N}$ signal is thought to be transported northwards to the ESTNP OMZ. Here, we present the first CCS sedimentary record of ladderane lipids, biomarkers for anammox, located within the ESTNP OMZ (32° N, 118° W). Over the last two glacial terminations (~ 160 kyr cal BP), ladderane concentrations were analysed in combination with the index of ladderanes with five cyclobutane moieties (NL₅), short-chain (SC) ladderane degradation products, and productivity proxies. This shows that (1) ladderanes were derived from anammox bacteria living within the ESTNP OMZ water column; (2) ladderanes were continuously present, with relatively high concentrations during both glacial and interglacial periods, showcasing that the ESTNP OMZ must have retained an anoxic core in which N loss occurred; and (3) anammox abundance appears to have been driven by both organic matter (OM) remineralization and advection changes, which regulated nutrient and oxygen levels. Our study shows that anammox was an important feature in the CCS, and it provides a more holistic picture of N-loss dynamics and the development of the ESTNP OMZ

over glacial–interglacial cycles. Lastly, ladderanes and their SC products were also detected in 160–500 kyr cal BP sediments (15.7–37.5 m b.s.f., metres below sea floor; analysed at a low temporal resolution), highlighting their potential as anammox biomarkers in relatively deeper buried sediments for future studies.

1 Introduction

The California Current system (CCS) is one of four major eastern boundary upwelling systems (known as EBUS). In EBUS, wind-driven offshore advection of surface waters causes deeper, cold, nutrient-rich waters to be upwelled into the photic zone, fuelling primary productivity (e.g. Bakun and Nelson, 1991). Consequently, the CCS is one of the world's most productive oceanic regions, with year-round upwelling, resulting in high primary production rates (Huyer, 1983; Dorman and Winanat, 1995). In the CCS, the respiration of sinking organic matter (OM), in combination with limited ventilation of the North Pacific intermediate waters (Reid and Mantyla, 1978; Sonnerup et al., 1999; Fine et al., 2001), results in the formation of the eastern North Pacific oxygen minimum zone (ENP OMZ). The ENP is divided into the eastern tropical North Pacific (ETNP) and the eastern subtropical North Pacific (ESTNP) OMZs.

The suboxic/anoxic conditions of OMZs cause the marine nitrogen (N) cycle to shift towards two processes that result in the loss of bioavailable N through the production of dinitrogen gas (N₂): (1) anaerobic ammonium oxidation

(anammox) and (2) denitrification. Anammox is the oxidation of ammonium (NH_4^+) to N_2 using NO_2^- as the terminal electron acceptor (van de Graaf et al., 1995, 1997), and it is performed in the marine water column by anammox bacteria of the genus *Candidatus Scalindua* (Kuypers et al., 2003). Anammox bacteria are chemolithoautotrophs and use carbon dioxide (CO_2) as their carbon source. Denitrification is the stepwise reduction of nitrate (NO_3^-) via nitrite (NO_2^-) to N_2 (Kuenen and Robertson, 1988) and is performed by a wide range of organisms, most of which are heterotrophs. During denitrification, nitrous oxide (N_2O) can be released as an intermediate product (Kuenen and Robertson, 1988), which has a global warming potential 265 times that of CO_2 (Vallero, 2019).

While permanent OMZs contribute to only 8 % of the total oceanic area (Paulmier and Ruiz-Pino, 2009), they are responsible for 20 %–50 % of total global N loss (Gruber, 2004; Codispoti et al., 2001). Decreased N availability in OMZs may limit primary producers and, hence, the uptake of CO_2 into the OM pool. This may reduce the efficiency of the ocean's biological pump, which exports organic C from the euphotic zone to the sea floor. Thus, OMZs not only have a disproportionately large impact on the marine nitrogen cycle, but changes in N-loss dynamics may also feed back into the carbon cycle.

The ENP OMZ is expanding both vertically (shoaling towards the ocean's surface; Bograd et al., 2008) and horizontally (Zhou et al., 2022) with present-day climate change. This follows observed trends of overall deoxygenation of the North Pacific since the 1960s (Whitney et al., 2007; Stramma et al., 2010; Pierce et al., 2012; Smith et al., 2022), linked to anthropogenically induced ocean warming as a response to increased greenhouse gas emissions (Laffoley and Baxter, 2019). As a result of the decreasing dissolved oxygen (DO) concentrations, denitrification has been shown to increase in the North Pacific over the last decades (Peters et al., 2018; White et al., 2019). Vertical expansion and intensification of the ENP OMZ have also occurred in the absence of anthropogenic influences in the past, as recorded by redox-sensitive trace metals in the sedimentary archive (Wang et al., 2020). This is thought to be caused by changes in DO concentrations during glacial–interglacial transitions (terminations). Model simulations indicate that during glacials cooling of the polar regions led to a more restrained and intensified Hadley cell (Nicholson and Flohn, 1980). This is thought to have caused southward transport of high-oxygen, nutrient-rich North Pacific Intermediate Water (NPIW; Herguera et al., 2010) and limited northward advection of the warm, oxygen-poor California Undercurrent (CU), resulting in a more oxygenated OMZ. During interglacials, the oxygen deficiency in the OMZ is thought to have increased due to enhanced advection of the warm, oxygen-depleted waters of the CU originating from the tropics (Lembke-Jene et al., 2018; Hendy and Kennett, 2003), water column stratification (Wang et al., 2020), and enhanced upwelling of nutrient-rich waters (Choumiline

et al., 2019). These previous glacial–interglacial transitions may be considered analogues for the effect of future climate change on the N cycle.

In the CCS, enriched isotope ratio values of bulk sedimentary nitrogen ($\delta^{15}\text{N}$) during interglacial periods have been interpreted to reflect increased denitrification in response to OMZ intensification (e.g. Kienast et al., 2002; Kemp et al., 2003; Liu et al., 2005). Sedimentary $\delta^{15}\text{N}$ values are governed by the isotopic fractionation (ϵ) induced by biological transformations and can be used to infer past N cycling. For water column denitrification, the production of N_2 induces an isotope fractionation effect of +20 ‰ to +30 ‰ on the residual nitrogen (Ryabenko, 2013; Sigman and Fripiat, 2019). Enrichment cultures of anammox bacteria have, however, shown that they induce a similar isotope fractionation effect (Brunner et al., 2013), with that of *Ca. Scalindua* spp. being +16 ‰ to +30 ‰ (Kobayashi et al., 2019). Although anammox occurs in the modern North Pacific oxygen-deficient waters (Rush et al., 2012a; Peng et al., 2015; Sollai et al., 2015; Hamasaki et al., 2018) and anammox is reported to be the dominant N-loss process in the eastern tropical South Pacific (ETSP; Galán et al., 2009; Thamdrup et al., 2006; Hamersley et al., 2007), to the best of our knowledge there are no reconstructions on the occurrence of anammox in the sediment archive of the CCS. Moreover, a long-standing conundrum is the discrepancy between the timing of enriched $\delta^{15}\text{N}$ values and enhanced marine productivity, especially north of the ETNP (Kienast et al., 2002), suggesting a decoupling between remineralization rates and N loss (Ganeshram et al., 2000).

While sedimentary $\delta^{15}\text{N}$ values are shaped by the sum of N-cycling processes, lipid biomarkers provide more detailed information (see Rush and Sinninghe Damsté, 2017, for a review). Anammox bacteria biosynthesize C_{18} and C_{20} ladderane fatty acids (FAs) (Fig. 1). These unique lipids contain three or five linearly concatenated cyclobutane rings ([3]-ladderane and [5]-ladderane, respectively; Sinninghe Damsté et al., 2002). Ladderanes have been successfully applied to trace abundances of *Ca. Scalindua* spp. in the modern ENP water column (Rush et al., 2012a; Sollai et al., 2015) and as anammox biomarkers in sedimentary records up to 140 ka (Jaeschke et al., 2009; Rush et al., 2019; van Kemenade et al., 2023). Moreover, during exposure to oxic conditions ladderane FAs undergo microbially mediated oxic degradation of the alkyl side chain by β -oxidation, in which C_{18} - and C_{20} -ladderane FAs are sequentially transformed into the short-chain (SC) C_{16} - and C_{14} -ladderane partial degradation products (Rush et al., 2011, 2012b). Thus, SC-ladderane FAs in the sediment archive may be used to trace back anammox cell material that has been exposed to oxic conditions, such as sedimentation through the oxic water underlying an OMZ. Furthermore, the index of ladderane FAs with five cyclobutane rings (NL_5) has been shown to correlate with the in situ water temperature at which ladderane FAs are synthesized (Ratray et al., 2010), which has been used to determine the

provenance of ladderane lipids (Jaeschke et al., 2009; Rush et al., 2012a; van Kemenade et al., 2022).

Here, we describe the occurrence of ladderane FAs in a ~ 160 kyr cal BP sediment record from the CCS, covering the two most recent glacial terminations (TI and TII). We combined (SC) ladderanes and the NL_5 index with sedimentary bulk $\delta^{15}N$, stable carbon isotope ratio ($\delta^{13}C$), total organic carbon (TOC), and total nitrogen (TN) to investigate the feedback of changing OMZ intensity on the occurrence of anammox within the CCS. Moreover, ladderane FAs were also investigated, albeit at a low resolution, in > 160 kyr cal BP sediments (up to 500 kyr cal BP) to explore their preservation potential.

2 Hydrographic setting

The northern boundary of the CCS is at the transition zone between the North Pacific Current (NPC) and Alaska gyres ($\sim 50^\circ N$) and is bordered in the south by the subtropical waters of Baja California, Mexico (~ 15 – $25^\circ N$). The CCS (Fig. 2a) is shaped by (i) the equatorward California Current (CC), extending roughly 1000 km off the North American coast (Checkley and Barth, 2009), (ii) the poleward nearshore-flowing CU, and (iii) the seasonal poleward-flowing Davidson Current (DC). The CC is a year-round, cold, low-salinity, nutrient-rich surface current (< 300 m b.s.s., metres below sea surface), originating from the North Pacific Current. While the CC is strongest in spring and summer, the DC originating around Point Conception ($35^\circ N$) dominates the surface-flow throughout winter. The deeper waters of the CC are shaped by the NPIW (300–800 m b.s.s.), which circulates clockwise in the North Pacific gyre (Sverdrup et al., 1942) and is carried southwards by the CC. Around Baja California, it convolutes with unventilated intermediate waters of tropical origin, which have been transported to the eastern Pacific by the Equatorial Undercurrent (EUC; Reid, 1997; Reid and Mantyla, 1978). Here, part of the CC turns north to become the CU. The CU (~ 100 – 300 m b.s.s.) carries the warm, high-salinity, low-oxygen waters from Baja California towards Vancouver Island (Thomson and Krassovski, 2010). Within the CCS, the geostrophic flow of the CC in combination with Ekman transport and eddy activity cause an offshore transport of (sub-)surface waters and strong coastal jets, which are replaced by the upwelling of the nutrient-rich undercurrent waters (Huyer, 1983; Chavez and Messié, 2009). Upwelling occurs year-round and results in high primary production (Bograd et al., 2009). In the CCS, the high organic matter flux, together with the poor ventilation of the intermediate-water mass (Reid and Mantyla, 1978; Fu et al., 2018), results in the formation of the ENP OMZ, disassociated into the ETNP (0 – $25^\circ N$; 75 – $180^\circ W$) and ESTNP (25 – $52^\circ N$; 75 – $180^\circ W$) (Fig. 2b). Dissolved oxygen (DO) concentrations in the cores ($< 20 \mu\text{mol kg}^{-1}$) of both the ETNP (~ 320 –

740 m b.s.s.) and ESTNP (~ 850 – 1080 m b.s.s.) OMZs decrease below $< 1 \mu\text{mol kg}^{-1}$ (Paulmier and Ruiz-Pino, 2009) (Fig. 2c).

3 Methods

3.1 Sampling location and strategy

The sediment record was recovered in 1996 during Ocean Drilling Program (ODP) Leg 167 (Lyle et al., 1997). Site 1012 is located 105 km offshore California in the East Cortez Basin ($32^\circ 16.970' N$, $118^\circ 23.039' W$), near the southern front of the CC and northern front of the ETNP OMZ (Fig. 2b). The core was recovered from a water depth of 1784 m b.s.s. For this study, 69 sediment depths (volumes of 20 cm^3) were selected for ladderane FA analysis. Sedimentation rates ranged from 4 to 15 cm kyr^{-1} (Table S1). Considering the oldest detected ladderane FAs were in 140 kyr sediments (~ 10 m b.s.f., below sea floor) of the Arabian Sea (Jaeschke et al., 2009), we subsampled at a higher resolution (every 10 to 50 cm) to the first ~ 160 kyr (15.7 m b.s.f.) of the record (with a maximum resolution of 10 cm around TI and TII) and at a lower resolution (80 to 200 cm) to ~ 500 kyr cal BP (37.5 m b.s.f.). In addition, 74 sediments (10–50 cm resolution) were analysed for bulk sedimentary TOC and TN contents, the C/N ratio (atomic), and bulk isotopic ratio values ($\delta^{15}N$ and $\delta^{13}C$). A detailed overview of all samples is given in the Supplement (Tables S1 and S2). Samples were freeze-dried and stored at $-20^\circ C$ prior to analysis.

3.2 Analysis of sedimentary bulk TOC, TN, C/N, $\delta^{13}C$, and $\delta^{15}N$

Sediments were freeze-dried and ground to powder. For TOC and $\delta^{13}C$ analyses, aliquots of bulk sediment were decalcified to remove all carbonates. Samples were first acidified with 2 M hydrochloric acid (HCl) and rinsed with distilled water to remove the salts. After the decalcification step, ca. 0.5 mg of dried material was used for the analysis. For TN and stable nitrogen isotope ratio ($\delta^{15}N$), between 15 and 20 mg of non-decalcified sediment was used. All samples were packed in tin cups and introduced to the Thermo Scientific Flash 2000 elemental analyser coupled to a Thermo Scientific Delta V Advantage isotope ratio mass spectrometer (EA/IRMS). Results are expressed in standard notation relative to Vienna Pee Dee Belemnite (VPDB) for $\delta^{13}C$ and relative to air for $\delta^{15}N$. The precision, as determined using laboratory standards, calibrated to certified international reference standards was in all cases $< 0.2 \text{ ‰}$. The sedimentary C/N ratios (based on total organic C and total N) were calculated using their atomic mass.

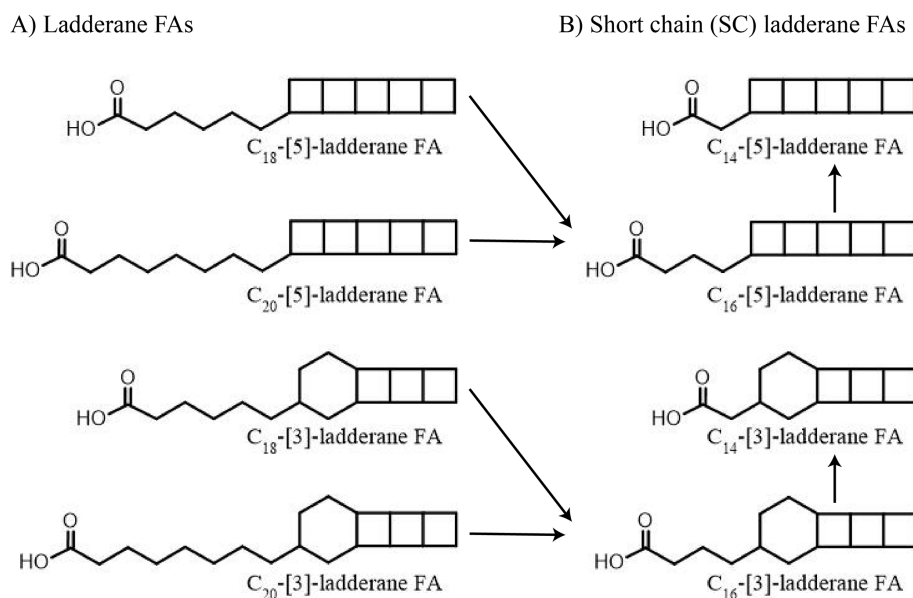


Figure 1. Structures of anammox lipid biomarkers used in this study: (a) ladderane fatty acids (FAs) with 5 or 3 cyclobutane moieties containing 18 or 20 carbon atoms. (b) Short-chain ladderane fatty acids (FAs) with 5 or 3 cyclobutane moieties containing 16 or 14 carbon atoms. Proposed diagenetic pathways are indicated using black arrows (adapted from Rush et al., 2011).

3.3 Age model

Liu et al. (2005) previously constructed an age model for ODP Site 1012, based on sediments recovered from Hole B. As the material used in this study is predominantly from Hole A and Hole C, a revised age model was constructed (Table S1). The revised age model for sediments up to 160 kyr cal BP (15.7 m c.d., metres composite depth) was created by correlation of the bulk sedimentary $\delta^{15}\text{N}$ record of Liu et al. (2005) with our dataset. Tie points (age vs. composite depth) were selected by fine-tuning using QAnalyseries (version 2022). For sediments > 160 kyr cal BP, which were solely sampled for ladderane FAs at low resolution (i.e. not sedimentary $\delta^{15}\text{N}$), the age model of Liu et al. (2005) was used. A more detailed description is provided in the Supplement (Sect. S1).

3.4 Ladderane extraction

Homogenized, freeze-dried sediments were extracted using a low-temperature low-pressure accelerated solvent extraction (ASE) method, previously described for ladderane extraction in Rush et al. (2012b). Thereafter, aliquots of the total lipid extract were saponified in 2 N potassium hydroxide (in a 96 % MeOH solution) by refluxing for 1 h. After, 2 mL of double-distilled water was added. The saponified extracts were acidified by adjusting the pH to 3 with 2 N hydrochloric acid (in a 50 % MeOH solution). Phase separation was induced by adding 2 mL of dichloromethane (DCM). The biphasic mixtures were sonicated for 5 min and centrifuged for 2 min (3000 rpm). The DCM layers, containing the FAs,

were collected. The mixtures were partitioned twice more with DCM, after which the same procedure was applied before collection of the DCM layers. The FA fractions were dried over a sodium sulfate (Na_2SO_4) column. Then, the fractions were methylated with diazomethane to convert FAs into their corresponding fatty acid methyl esters (FAMES) and allowed to air-dry overnight to avoid losing the more volatile SC-ladderane FA had they been dried under a stream of N_2 . The methyl esters of the polyunsaturated fatty acids (PUFAs) were removed by eluting the FAME fractions with DCM over a silica-impregnated silver nitrate (AgNO_3) column. FAME fractions were dissolved in acetone and filtered over 0.45 mm PTFE filters (4 mm; BGB, USA).

3.5 Ladderane analysis

A commercially available deuterated $\text{C}_{20}[5]$ -PUFA (Reagecon Diagnostics Ltd) was added as an internal standard to the FAME fractions. FAME fractions were analysed on an Agilent 1290 Infinity I ultra-high-performance liquid chromatographer (UHPLC), equipped with a thermostatted autoinjector and column oven, coupled to a Q Exactive Plus Orbitrap MS, with an atmospheric pressure chemical ionization (APCI) probe (Thermo Fischer Scientific, Waltham, MA) operated in positive ion mode. Separation was achieved with a Zorbax Eclipse XDB C_{18} column (Agilent, 3.0×250 mm, $5 \mu\text{m}$), using MeOH as an eluant (0.4 mL min^{-1}). APCI source settings were set as follows: corona discharge current, $2.5 \mu\text{A}$; source CID (collision-induced dissociation), 10 eV ; vaporizer temperature, $475 \text{ }^\circ\text{C}$; sheath gas flow rate, 50 arbitrary units (AU); auxiliary gas flow rate, 30 AU; capillary

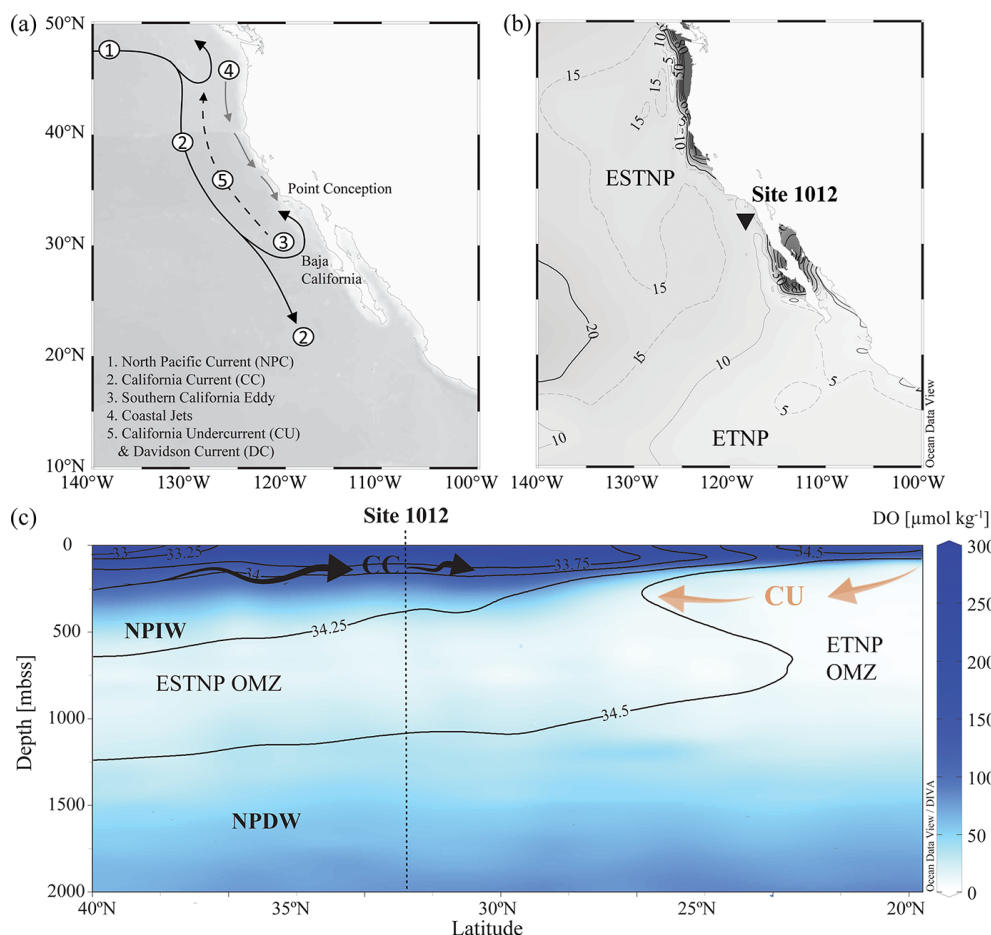


Figure 2. (a) Map of the California Current system (CCS). Key currents are indicated with arrows. (b) Location of ODP Site 1012 ($32^{\circ}16.970^{\circ}\text{N}$; $118^{\circ}23.039^{\circ}\text{W}$) recovered at 1784 m b.s.s., with minimum dissolved oxygen (DO) concentrations [$\mu\text{mol kg}^{-1}$] detected in the water column in 2018 (Garcia et al., 2019). (c) A latitudinal section plot of the CCS water column showing modern annually averaged DO ($\mu\text{mol kg}^{-1}$) concentrations and salinity (psu) concentrations with the colour bar and contour lines, respectively (Garcia et al., 2019). Major current and water masses are also indicated, i.e. the eastern tropical and eastern subtropical North Pacific (ETNP and ESTNP, respectively) OMZs, the California Current (CC; black arrows), the California Undercurrent (CU; orange arrows), North Pacific Intermediate Water (NPIW), and North Pacific Deep Water (NPDW). Maps were created in Ocean Data View and DIVA gridding was applied for interpolation of DO concentrations (Schlitzer, Reiner, Ocean Data View, <https://odv.awi.de> (last access: 4 December 2023), 2021).

temperature, 300°C ; and S-lens, 50 V (van Kemenade et al., 2022). A mass range of m/z 225–380 was monitored (resolution 140 000 ppm), followed by data-dependent MS^2 (resolution 17 500 ppm at m/z 200), in which the 10 most abundant masses in the mass spectrum were fragmented successively (stepped normalized collision energy 20, 25, 30 eV). An inclusion list containing the exact masses of C_{14-24} [3]- and C_{14-24} [5]-ladderane FAMES was used. Mass chromatograms (within 5 ppm mass accuracy) of the protonated molecules ($[\text{M}+\text{H}]^+$) were used to integrate the detected ladderanes: C_{14} [3]-, C_{14} [5]-, C_{16} [5]-, C_{18} [3]-, C_{18} [5]-, C_{20} [3]-, and C_{20} [5]-ladderane FAMES (m/z 235.169, 233.154, 261.185, 291.232, 289.216, 319.263, and 317.248, respectively), as well as the internal deuterated C_{20} [5]-PUFA standard (m/z 322.279). A detection limit of 30–35 pg injected

on-column and a linear response of ($r(4) > 0.99$) over approximately 3 orders of magnitude was achieved (Table S8). Identification of ladderanes was achieved by comparing retention times and spectra with in-house isolated C_{20} [3]- and C_{20} [5]-ladderane FAME standards (Hopmans et al., 2006; Rattray et al., 2008) and with ladderane FAMES in a biomass sample of *Ca. Kuenenia*.

Previously, ladderane FAME quantification has been conducted using calibration curves of in-house isolated C_{20} [3]- and C_{20} [5]-ladderane standards (Hopmans et al., 2006). However, this quantification method does not correct for any variability in ion intensity, due to, for example, matrix effects and/or changes in the instruments functioning. Therefore, we further optimized this quantification method to include a response correction using a commercially avail-

able internal standard (deuterated C₂₀[5]-PUFA). At the start of each sequence, calibration curves were made for the C₂₀[3]- and C₂₀[5]-ladderane standards and the deuterated C₂₀[5]-PUFA standard. The relative response of the deuterated C₂₀[5]-PUFA commercial standard in relation to the ladderane FAME standards was determined from the slopes of their calibration curves (giving a relative response factor, i.e. RRF). An RRF of 1.3 was used for [3]-ladderanes, based on the C₂₀[3]-ladderane, and an RRF of 1.2 for the [5]-ladderanes, based on the C₂₀[5]-ladderane. Using the RRFs, ladderane FAME concentrations (C_L , expressed in $\mu\text{g g}^{-1}$ dry weight) were calculated as follows:

$$C_L = \frac{m_{\text{IS}} \left(\frac{A_L}{\left(\frac{A_{\text{IS}}}{\text{RRF}} \right)} \right)}{m_S}, \quad (1)$$

with m_{IS} being the mass (μg) of the added internal standard, m_S the dry weight of extracted sediment (g), A_L the integrated peak area of the given ladderane FAME, A_{IS} the integrated peak area of the internal standard, and RRF the relative response factor. Ladderane concentrations (including concentrations normalized against gram TOC) are reported in the Supplement (Tables S4 and S5). To compare with previous studies that did not use an internal standard, the established method that uses external calibration curves of three authentic standards (Hopmans et al., 2006; Rush et al., 2012b; Rattray et al., 2010) was also performed (Table S9). A comparison between both quantification methods is provided in the Supplement (Sect. S2).

3.6 NL₅ index

The index of ladderane lipids with five cyclobutane rings (NL₅) correlates with the temperature at which they were synthesized. The NL₅ index is calculated according to the following equation:

$$\text{NL}_5 = \frac{C_{20}[5]\text{ladderane FA}}{C_{18}[5]\text{ladderane FA} + C_{20}[5]\text{ladderane FA}} \quad (2)$$

The empirical fourth-order sigmoidal relationship between the NL₅ index and temperature is then described by

$$\text{NL}_5 = 0.2 + \frac{0.7}{1 + e^{-\left(\frac{T-16.3}{1.5}\right)}}, \quad (3)$$

with temperature (T) in $^{\circ}\text{C}$ (Rattray et al., 2010).

3.7 Degradation rates and constants

Ladderane concentrations over the entire record (Fig. 3) were used to calculate ladderane degradation rates, with the following equation for lipid degradation (Canuel and Martens, 1996):

$$k' = \frac{-\ln\left[\frac{C_t}{C_{t_0}}\right]}{t}, \quad (4)$$

with k' being the first-order rate constant (kyr^{-1}), C being the concentration ($\mu\text{g g}^{-1}$ dry weight) at time t (C_t) and at the initial time (C_{t_0}), and t being the relative time (kyr). Ladderane degradation constants and rates are provided in the Supplement (Table S7).

4 Results

4.1 Bulk sedimentary total nitrogen and total organic carbon

Bulk sedimentary total nitrogen (TN) ranged between 0.1 %–0.6 % throughout the record. $\delta^{15}\text{N}$ fluctuated from 5.8 ‰ to 10.0 ‰. An offset of 3 ‰ to 4 ‰ was observed between interglacials and glacials, with higher values during interglacials. Sedimentary total organic carbon (TOC) varied between 1.7 %–7.4 % throughout the record, whilst its carbon isotopic composition ($\delta^{13}\text{C}_{\text{TOC}}$) ranged from -23.0 ‰ to -21.6 ‰. C/N ratios (atomic) ranged from 13 to 23 (Fig. 4f–j; Table S3).

4.2 Ladderane FA concentrations and the NL₅ index

The ladderane fatty acids identified in this record were C₁₈[5]-, C₁₈[3]-, C₂₀[5]-, and C₂₀[3]-ladderanes, and their diagenetic products were the SC C₁₄[5]-, C₁₄[3]-, and C₁₆[5]-ladderanes. Summed SC-ladderane and ladderane concentrations over the entire 500 ka record were 0.5–33 and 0.1–23 ng g^{-1} dry weight, respectively (Fig. 3; Table S5). Normalized concentrations over the 160 ka record ranged as follows: C₁₄[5]-ladderane 16–158 ng g TOC^{-1} , C₁₄[3]-ladderane 27–184 ng g TOC^{-1} , C₁₆[5]-ladderane 34–198 ng g TOC^{-1} , C₁₈[5]-ladderane 7–107 ng g TOC^{-1} , C₁₈[3]-ladderane 4–76 ng g TOC^{-1} , C₂₀[5]-ladderane 5–79 ng g TOC^{-1} , and C₂₀[3]-ladderane 10–208 ng g TOC^{-1} (Fig. 4b, c; Table S4). Concentrations calculated without the use of the internal standard (Hopmans et al., 2006; see Sect. 2.5) are reported in the Supplement (Table S9) and were a factor of 1.2 and 1.3 lower for [3]- (SC-)ladderanes and [5]- (SC-)ladderanes, respectively. Concentrations calculated with the two quantification methods showed a strong positive linear relationship of $R^2 = 0.88$ and 0.89 for [3]- (SC-)ladderanes and [5]- (SC-)ladderanes, respectively (Fig. S2). The NL₅ index (Eq. 2) ranged from 0.3 to 0.8 throughout the record. Corresponding NL₅-derived temperatures (Eq. 3) were between 13.1–18.6 $^{\circ}\text{C}$, with highest values observed in the > 160 kyr cal BP sediments (Table S6).

5 Discussion

In the sediment record of ODP Site 1012, C₁₈[3]-, C₁₈[5]-, C₂₀[3]-, and C₂₀[5]-ladderane FAs and their short-chain C₁₄[3]-, C₁₄[5]-, C₁₆[5]-ladderane products were detected over the last 500 kyr (~ 38 m.b.s.f.; Fig. 3). This poses

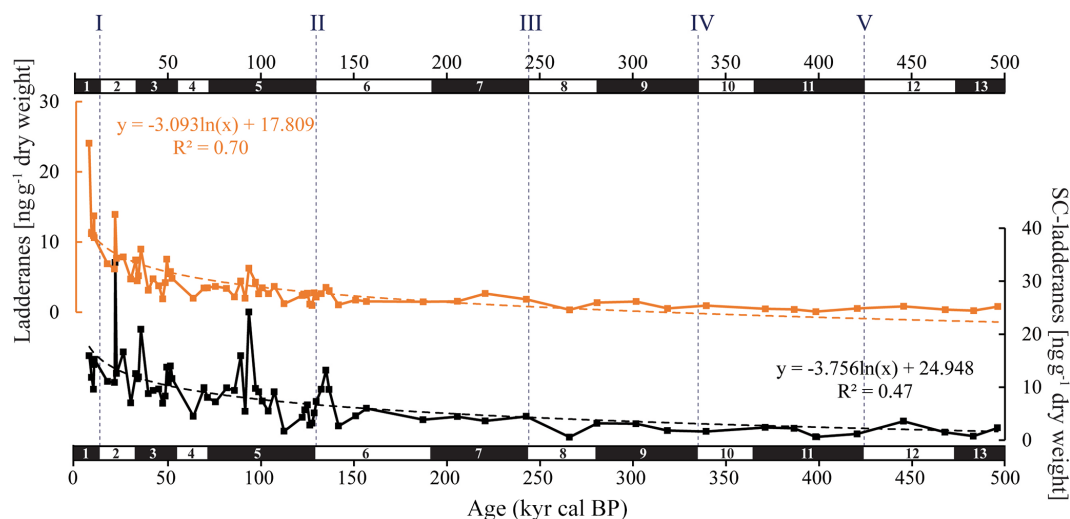


Figure 3. Summed $C_{18}[5]-$, $C_{18}[3]-$, $C_{20}[5]-$, and $C_{20}[3]-$ ladderane (orange) and summed short-chain (SC) $C_{14}[5]-$, $C_{14}[3]-$, and $C_{16}[5]-$ ladderane (black) concentrations (ng g^{-1} dry weight) in the ODP Site 1012 record. The logarithmic relationship between ladderanes and SC ladderanes with time is provided (with corresponding R^2) and is displayed with orange and black dashed lines, respectively. Grey dashed lines indicate the approximate timing of glacial terminations I to V. Note that the scales of the y axes are different.

a considerable extension of the ladderane record (formerly detected up to ~ 140 ka BP in Arabian Sea sediments; ~ 10 m b.s.f.; Jaeschke et al., 2009). Below, we will first discuss the provenance of the detected ladderane lipids (Sect. 5.1). Then, their variability throughout glacial–interglacial cycling will be discussed (Sect. 5.2), ending with the subsequent implications on our understanding of the nitrogen cycle of the CCS (Sect. 5.3). Unfortunately, the coarse sampling resolution in the > 160 kyr cal BP sediments and low ladderane FA concentrations (due to diagenesis) complicate interpretations of ladderane FA fluctuations in these sediments. Therefore, analysis of trends in ladderane concentrations over (inter)glacial cycling is limited to the < 160 kyr cal BP sediments.

5.1 Ladderanes sourced from anammox bacteria in the ESTNP OMZ water column

The relative contribution of SC ladderanes to the total ladderane pool is a measure of oxygen exposure (Rush et al., 2011, 2012b), and the NL_5 index is a measure of the water temperature of the niche of anammox bacteria (Ratray et al., 2010). In combination, these data may provide insights into the origin of ladderanes in the CCS sediment record.

In the CCS, a progressive depletion of both the water column $\delta^{15}\text{N}_{\text{NO}_3}$ and sedimentary $\delta^{15}\text{N}$ signal occurs with increasing latitude, resulting in more depleted values at ODP Site 1012 (8‰–10‰; Altabet et al., 1999; Liu et al., 2005; this study) than in the ETNP OMZ core. The northward transport of denitrified waters by the poleward-flowing oxygen-poor CU from the core of the ETNP has been evoked to explain this trend (Castro et al., 2001; Kienast et al., 2002). This means that at ODP Site 1012, the sedimentary $\delta^{15}\text{N}$ sig-

nal is thought to predominantly derive from the ETNP and not the ESTNP OMZ. In order to understand the observed ladderane trends in the ODP Site 1012 record, it is thus important to establish whether the detected ladderanes reflect a local signal (from the ESTNP OMZ) or whether they are also sourced from the ETNP OMZ core and similarly transported northwards with the CU, towards ODP Site 1012. Alternatively, ladderanes could also be synthesized by sedimentary anammox bacteria (Vossenberg et al., 2008).

At ODP Site 1012, SC ladderanes were present at relative abundances of 40%–88% throughout the record (Fig. 4d). Ladderane FAs are relatively labile compounds, and in the Arabian Sea they have been shown to already degrade into their SC products (at relative proportions of $\sim 20\%$) within the OMZ water column ($\text{DO} < 3 \mu\text{mol L}^{-1}$). There, the sinking of ladderanes through the oxygenated bottom waters underlying the OMZ ultimately resulted in similar relative abundances of SC ladderanes in the surface sediments of 20%–80%, depending on water column depth (Rush et al., 2012b). The similarly high contribution of SC ladderanes in the ODP Site 1012 record suggests that ladderanes are also sourced from an overlying OMZ water column (i.e. the ESTNP OMZ) and sunk through oxygenated bottom waters before being deposited on the seafloor, which readily became anoxic in view of the high TOC content (Fig. 4j).

An OMZ water column source is consistent with the NL_5 index (0.3–0.8; Fig. 4e). According to the NL_5 calibration by Ratray et al. (2010), NL_5 indices within this range more closely reflect water column rather than sedimentary anammox bacteria. Also, NL_5 -derived temperatures (13–17 °C; Table S6) are significantly higher than what would be expected for sea-floor temperatures (i.e. modern annual aver-

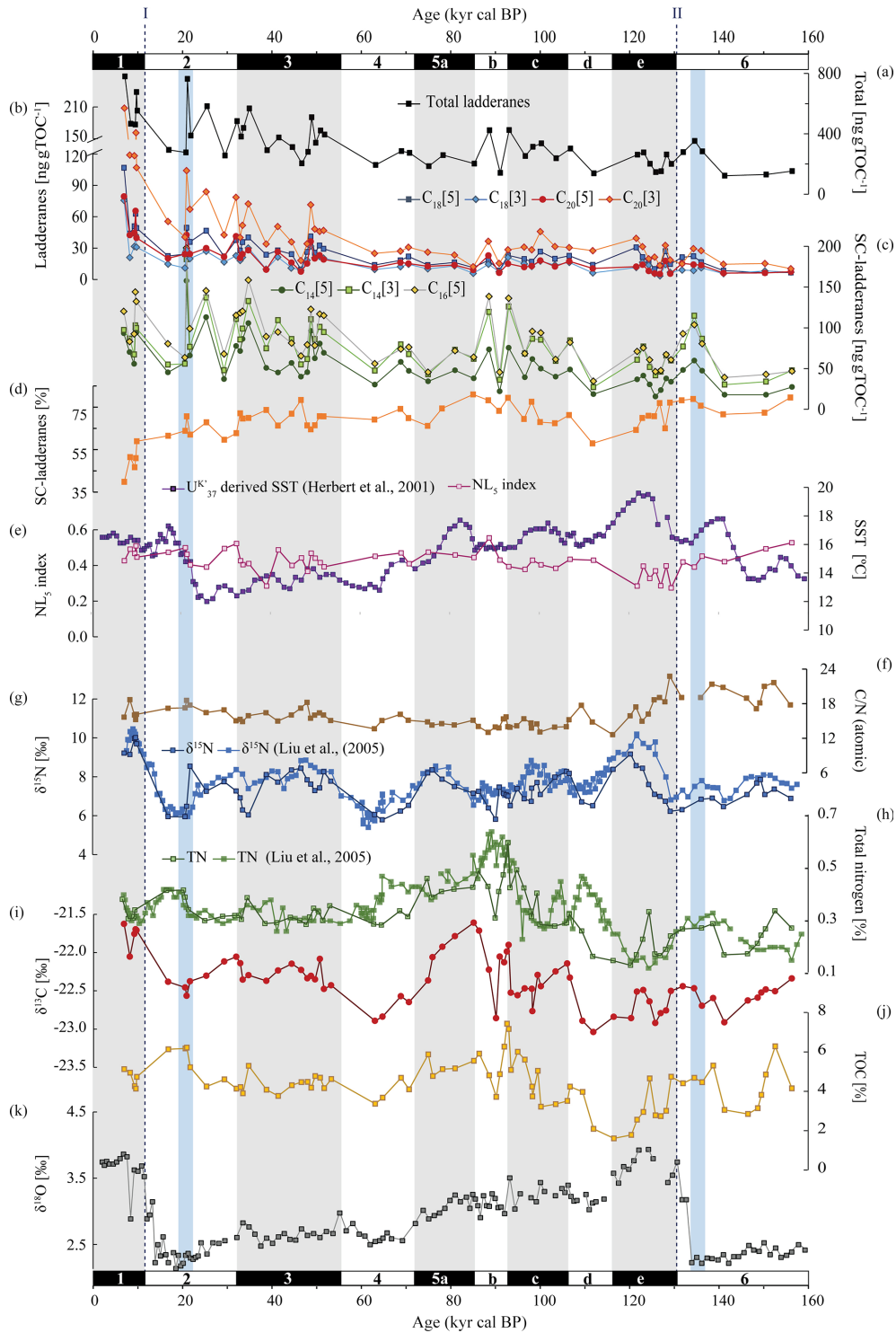


Figure 4. From top to bottom: concentrations of (a) total ladderanes (summed SC ladderanes and ladderanes), (b) ladderanes, and (c) SC ladderanes (normalized against TOC [ng g TOC⁻¹]), (d) relative abundance of SC ladderanes over total ladderanes [%], (e) $U_{37}^{K'}$ -derived sea-surface temperatures (SSTs) from Herbert et al. (2001) [°C] and the NL₅ index from this study, (f) atomic ratio of total organic carbon (TOC) over total nitrogen (TN), (g) bulk sedimentary $\delta^{15}\text{N}$ from Liu et al. (2005) and this study [‰], (h) TN from Liu et al. (2005) and this study [%], (i) bulk sedimentary $\delta^{13}\text{C}$ [‰], (j) TOC [%] and (k) benthic $\delta^{18}\text{O}$ record from Herbert et al. (2001) [‰]. All data are derived from the same location (ODP Site 1012). Marine isotope stages (known as MIS) are indicated with black and white bars. Periods of maximum global ice volume (Herbert et al., 2001; blue bars) and the approximate timing of glacial terminations TI and TII (dashed lines) are also indicated.

age bottom water temperatures at Site 1012 are $< 5^{\circ}\text{C}$; Garcia et al., 2019). Additionally, while the transport of ladderane FAs has been shown to occur within oxygen-depleted systems (van Kemenade et al., 2022), long-distance transport of ladderane FAs with the CU (characteristic DO concentration of $\sim 62\ \mu\text{mol L}^{-1}$ in modern CU water; Sahu et al., 2022) is unlikely, and it would be expected to yield higher relative abundances of SC-ladderane FAs than detected in the record. Transport of ladderanes is also not reflected in present-day ENP ladderane distributions, as an investigation of ladderanes at more northerly ($\sim 20^{\circ}\text{N}$) and more southerly ($\sim 17^{\circ}\text{N}$) located sites showed in situ synthesis by pelagic *Ca. Scalindua* at both sites (Sollai et al., 2015). Hence, ladderane FAs are thought to predominantly derive from the ESTNP OMZ water column and reflect a local anammox signal, although some contribution of allochthonous or sedimentary anammox cannot be entirely excluded.

5.2 Anammox variability in the CCS over the last 160 kyr

5.2.1 The Holocene and MIS 5, including the penultimate interglacial of MIS 5e

Over the ~ 500 kyr cal BP record, ladderane FAs are observed to decrease logarithmically with time (Fig. 3; $R^2 = 0.70$), in which the degradation constant k follows a linear relationship (when logarithmically transformed; Fig. 5a; $R^2 = 0.88$) with time. This is consistent with first-order degradation kinetics, typical for OM (Canuel and Martens, 1996). As such, it is not surprising that the highest ladderane concentrations are observed in the youngest sediments, deposited during the early to mid-Holocene. Even so, ladderane FAs normalized against TOC also show elevated concentrations in Holocene sediments. This suggests that high ladderane FAs at this time are not simply a preservation signal but also reflect an increase (compared to pre-Holocene sediments) in their production by *Ca. Scalindua* spp. relative to the total organic C pool. Moreover, elevated ladderanes in the early to mid-Holocene sediments coincide with enriched bulk $\delta^{15}\text{N}$ (9‰–10‰; Fig. 4g), indicative of enhanced N loss by anaerobic microorganisms, and elevated TOC and TN concentrations (Fig. 4h, j), indicative of increased productivity.

In contrast to ladderane FAs, concentrations of their SC products are not highest in Holocene sediments. Consequently, the SC-ladderane data do not fit the logarithmic decrease with time well ($R^2 = 0.47$; Fig. 3), which is also reflected in the relationship of the degradation constant k with time (Fig. 5a; $R^2 = 0.43$). The oxidation of ladderane FAs to produce SC-ladderane FAs (Rush et al., 2011) has been shown to take place within the oxic waters below the OMZ. In this way, 20%–80% of the ladderane FAs were transformed into SC ladderanes in the Arabian Sea (Rush et al., 2012c). Throughout the deeper CCS sedimentary record

(> 10 kyr cal BP), the relationship between ladderane FAs and their SC products follows a linear trend ($R^2 = 0.87$; Fig. 5b), with SC ladderanes making $\sim 60\%$ – 80% of total ladderanes (Fig. 4d). However, in Holocene sediments (< 10 kyr cal BP), the relationship between ladderanes and SC ladderanes is different (Fig. 5b), and SC-ladderanes occur at relatively lower abundance (40%–60%) compared to the rest of the record. This indicates that, after 10 kyr cal BP, there was no significant change in the exposure of ladderane FAs to the oxygenated water underlying the ETNP OMZ before being buried in the sediment record, but that in the recent record there was reduced oxygen exposure.

Reduced oxygen exposure is likely to have resulted from an intensified OMZ; Lembke-Jene et al. (2018) showed, using paleoceanographic proxies and paleomodelling, that a combination of sea ice loss, increased SST, and remineralization rates led to more deoxygenated intermediate waters (the NPIW) during the early to mid-Holocene in the North Pacific. Moreover, in the ETNP, enriched sedimentary $\delta^{15}\text{N}$ values and laminated sediments during the early Holocene, alongside geochemical tracers, have been interpreted to signal the presence of a strong OMZ at this time, while bioturbated sediments occurred over the last glacial period (Thunell and Kepple, 2004).

Ladderane FA concentrations also peak during the penultimate interglacial (the Eemian; MIS 5e), in line with enriched (> 8‰) $\delta^{15}\text{N}$ values. Microfossil data from MIS 5 have indicated that intermediate waters in the western North Pacific were more deoxygenated during the Eemian (Matul et al., 2016), which may have driven increased anammox in the CCS at this time. Yet, while $\delta^{15}\text{N}$ values over MIS 5 maximize during MIS 5e, ladderane FA concentrations peak during mid-MIS 5 (MIS 5b–c). During MIS 5b–d, when (SC-)ladderane FA concentrations maximize, intermediate waters in the western North Pacific were likely oxic (Matul et al., 2016), and the $\delta^{15}\text{N}$ signal is more subdued (< 8‰; Fig. 4g). At this time, increased (SC-)ladderane FAs coincide with peaks in paleo-productivity proxies (i.e. TOC and TN; Fig. 4h, j). Over the course of MIS 5, from late MIS 5e onwards, SSTs in the CCS decreased while the CC strengthened (Herbert et al., 2001; Yamamoto et al., 2007). This would have led to increased transport of high-oxygen, nutrient-rich NPIW (Herguera et al., 2010) and enhanced open ocean upwelling. This may have fuelled productivity, which explains the high TOC and TN concentrations in mid-MIS 5.

The C/N ratio remains fairly stable throughout MIS 1 to MIS 5c (mean MN = 16, standard deviation SD = 2; Fig. 4f), with higher values observed during MIS 6 (MN = 20, STD = 2; discussed in Sect. 5.2.2). Based on stoichiometry, enhanced NO_3^- supply is expected to lower the ratio in phytoplankton biomass (Matsumoto et al., 2020). Yet, changes in nutrient concentrations have been observed to effect the C/P and N/P ratios but not the C/N ratio (Frigstad et al., 2011). It is therefore not surprising that the increased TN content during mid-MIS 5 is not reflected in the C/N ratio. Also, while

the $\delta^{13}\text{C}$ signal (-23% to -22% ; Fig. 4I) reflects a typical marine origin of OM, the C/N ratio is higher than commonly observed for marine algae (e.g. Lamb et al., 2006). This is likely caused by preferential remineralization of organic N during the settling of OM from the photic zone (Verardo and McIntyre, 1994; Schneider et al., 2003).

During mid-MIS 5, where TN and TOC peak, anammox may have been fuelled by local increases in OM. Babbín et al. (2014) showed, using incubations from the ETNP OMZ, that anammox rates increase in response to the addition of OM. Likewise, in the modern Southern Pacific OMZ, N loss by anammox was found to be strongly correlated with the export of OM, via the release of ammonium into the water column through remineralization (Kalvelage et al., 2013). As such, the co-occurrence of ladderane FA and paleo-productivity proxy maxima during MIS 5 could reflect an increase in *Ca. Scalindua* spp. abundance in response to an increased N-substrate supply via OM remineralization or nutrient transport. Remineralization of increased phytoplankton biomass may consequently also have led to more reduced local conditions, which would also favour anammox. This local signal would not have been recorded in the western part of the North Pacific, where intermediate waters were oxic (Matul et al., 2016). The relatively subdued $\delta^{15}\text{N}$ signal during mid-MIS 5 and consequent implications for our understanding of the N cycle in the CCS are further discussed in Sect. 5.3.

5.2.2 The two most recent glacial periods

Ladderane FAs are observed to increase from early MIS 3 to mid-MIS 2 and from the middle to late MIS 6. Maxima of ladderanes occur approximately at the timing of ice sheet volume maxima of the last glacial maxima (LGM) and the penultimate glacial of MIS 6 (blue bars in Fig. 4; following timing of Herbert et al., 2001). During the last glacial period ($\sim 115\text{--}12\text{ ka}$) and the penultimate glacial MIS 6, large parts of the North American continent were covered by the Laurentide and Cordilleran ice sheets. While glacials are typically associated with a well-ventilated intermediate-water mass (Herguera et al., 2010) and a strong southward advection of the CC (Ortiz et al., 1997), a weakening of the CC has been proposed to occur at times of global ice sheet maxima. In the CCS, $U_{37}^{K'}$ -derived temperatures indicate that SSTs increased $\sim 12\text{ kyr}$ in advance of maximal ice sheet volumes. This is thought to reflect increased northward advection of warm oxygen-poor waters carried by the CU and DC in response to a weakened CC due to large ice sheet volumes (Herbert et al., 2001). Using trace elements, Cartapanis et al. (2011) found that intermediate water oxygenation off Baja California deteriorated slightly over the course of late MIS 3 and early MIS 2, consistent with a strengthening of the CU at this time. As such, the increased abundance of ladderanes observed during (and leading up to) ice sheet maxima at ODP Site 1012 may derive from an increased *Ca. Scalindua* spp.

abundance due to more reduced local conditions, via the enhanced strength of the CU.

MIS 6 and its termination (TII) are further characterized by relatively high C/N ratios (17–23; Fig. 4f). Matsumoto et al. (2020) found, using a global ocean carbon cycle model, that during glacial periods the expansion of sea ice increased global C:N:P ratios. Additionally, taxonomic changes during glacials, in which eukaryotic phytoplankton became more dominant, resulted in NO_3^- depletion (hereby increasing the C/N ratio). At the same time, decreased upwelling during glacial periods in the North Pacific (Worne et al., 2019) may have also lowered nutrient availability. Low N availability is reflected in relatively low TN concentrations in this record (Fig. 4h). This suggests anammox at this time was primarily promoted by reduced local DO concentrations via enhanced CU strength rather than enhanced nutrient supply and/or increased remineralization rates.

While enhanced anammox in response to deoxygenation during glacial maxima is at odds with previous assessments of N loss in the CCS (e.g. Liu et al., 2005), deoxygenation of the Pacific is consistent with recent paleo-proxy studies (Lu et al., 2016; Anderson et al., 2019) and modelling results (Matsumoto et al., 2020). According to these studies, many parts of the glacial ocean, including the equatorial Pacific, had substantially lower DO during the last glacial period than today. This fits with increased ladderane FAs at this time, which suggests N loss in the CCS was likely more intense during glacial maxima than previously assumed.

5.3 Implications of the occurrence of anammox on the N cycle in the CCS

In the CCS, previous estimates of changes in N loss over time have been based on the bulk sedimentary $\delta^{15}\text{N}$ record. Enriched $\delta^{15}\text{N}$ during interglacials (7%–10%) are thought to reflect intensified denitrification in response to reduced DO, while more depleted $\delta^{15}\text{N}$ during glacials (4%–6%) are assumed to reflect lowered rates in response to increased DO (Liu et al., 2005, 2008). However, the occurrence of ladderane FAs throughout our CCS record now shows that anammox was (also) responsible for N loss and thus contributed, at least partially, to the sedimentary $\delta^{15}\text{N}$ record.

The cross-correlation for both $\delta^{15}\text{N}\text{--}\delta^{18}\text{O}$ and $\delta^{18}\text{O}\text{--}\text{SST}$ at ODP Site 1012 (Liu et al., 2005) indicates that fluctuations in $\delta^{15}\text{N}$ occur in tandem with glacial–interglacial cycling. However, a long-standing conundrum has been the discrepancy between the $\delta^{15}\text{N}$ record and productivity proxies (i.e. TOC and TN), especially north of the ETNP (Kienast et al., 2002), as also seen in our record (Fig. 4). This decoupling has been used previously to suggest that variations in denitrification were not due to changes in OM remineralization rate but rather from changes in ocean circulation and ventilation patterns (Ganeshram et al., 2000). Yet, fluctuations in ladderanes *do* seem to follow trends in paleo-productivity proxies (i.e. TOC and TN) relatively closely, especially during the

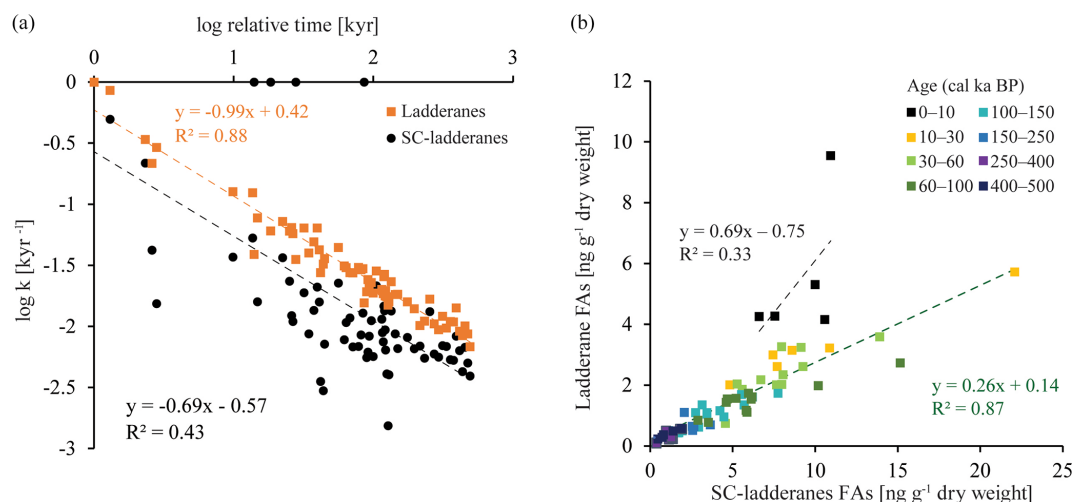


Figure 5. (a) Linear relationship between the logarithmic values of the degradation constant k and relative time for ladderane FAs (orange squares) and SC-ladderane FAs (black dots). (b) Relationship between ladderane FAs and SC-ladderane FAs, in which samples are colour-coded according to age. The linear relationship and corresponding R^2 are given for the most recent age group (0–10 kyr cal BP; in black) and the > 10 kyr cal BP age groups (in green).

Holocene, MIS 3, and MIS 5. And, while enriched $\delta^{15}\text{N}$ values sometimes correspond to ladderane maxima (i.e. during the Holocene), discrepancies with ladderane concentrations are seen especially during MIS 5 and during glacial periods (Fig. 4).

This may suggest that increased anammox does not always correspond to increased N loss, possibly via simultaneously reduced denitrification rates (Koeve and Kähler, 2010). Yet, Babbín et al. (2014) showed, using incubations from the ETNP OMZ, that both denitrification and anammox are limited by OM supply, and their rates increase in response to the addition of OM. Moreover, these authors showed that both denitrifiers and anammox bacteria are similarly inhibited by oxygen in the marine environment, at DO concentration around 3 to $8\ \mu\text{mol L}^{-1}$ (Babbín et al., 2014). As such, both anammox and denitrification should respond similarly to changes in DO and OM in the CCS.

Moreover, given the average C/N signature of marine OM (106:16; Redfield et al., 1963), stoichiometric constraints should result in a ratio of N_2 production via denitrification and anammox of 71:29 (Koeve and Kähler, 2010). On the one hand, this means that the relative contribution of anammox to N_2 production is likely lower than the contribution of denitrification, possibly resulting in a less strong influence of anammox on the $\delta^{15}\text{N}$ signal. On the other hand, this means that denitrification and anammox rates should be positively related, in which increased anammox is associated with increased denitrification (Koeve and Kähler, 2010). Potentially, anammox and denitrification could be unsynchronized (as indicated by differences between the ladderane and $\delta^{15}\text{N}$ records) in response to variations in the C/N ratio of OM. Localized variations in the C/N signature may result in different relative contributions. Yet, integrating these varia-

tions over space and time should obtain a similar ratio (Dalsgaard et al., 2012; Babbín et al., 2014; Ward, 2013). Additionally, the C/N ratio remains fairly consistent throughout the record (13–19), except during MIS 6 where it is higher (17–23; Fig. 4f) and variations do not correspond to those observed in ladderane FAs or $\delta^{15}\text{N}$. As such, given the temporal resolution of the record (which does not cover seasonality), denitrification and anammox intensities are expected to fluctuate in tandem.

Consequently, variability in $\delta^{15}\text{N}$ of the CCS sedimentary record may, at times, simply not relate directly to changes in denitrification and/or anammox rates. Reconstructions of N loss using sedimentary $\delta^{15}\text{N}$ depend on the assumption that there was complete biological utilization of NO_3^- by phytoplankton. However, during periods of high upwelling intensity (as likely occurred during mid-MIS 5; see Sect. 5.2.1), the high NO_3^- availability may result in incomplete NO_3^- assimilation. This allows for the preferential uptake of ^{14}N by primary producers, resulting in a pool of $\delta^{15}\text{N}$ depleted OM available for heterotrophic denitrification (Tesdal et al., 2013). Hence, at times of high NO_3^- supply, incomplete nitrate assimilation would have quenched the $\delta^{15}\text{N}$ signal, even if denitrification was as intense as during periods of low NO_3^- availability. Moreover, a study by Altabet and Francois (1994) showed that sedimentary $\delta^{15}\text{N}$ in the equatorial Pacific records the isotopic enrichment of near-surface NO_3^- via depletion by phytoplankton, in which enriched $\delta^{15}\text{N}$ values are associated with reduced NO_3^- availability for phytoplankton assimilation. Also, in the South Pacific, NO_3^- concentrations have been found to affect the $U_{37}^{K'}$ index (Mercer et al., 2005). Given the phase relationship between the $\delta^{15}\text{N}$ and $U_{37}^{K'}$ -based SST records of the CCS (Liu et al., 2008) and the discrepancies between the $\delta^{15}\text{N}$ and

ladderane records, it may be reasonable to conclude that the CCS sedimentary $\delta^{15}\text{N}$ fluctuations (also) record variations in NO_3^- assimilation by phytoplankton.

Additionally, other biological processes may influence the $\delta^{15}\text{N}$ signal (Zonneveld et al., 2010). In the Gulf of Tehuantepec, at the southern end of the ETNP OMZ core, $\delta^{15}\text{N}$ values decrease over the course of the Holocene (Thunell and Kepple, 2004; Hendy and Pedersen, 2006), while laminated sediments suggest reduced DO concentrations. This was interpreted as being the result of increased N_2 fixation ($\varepsilon: \leq +2\%$; Sigman and Fripiat, 2019), which lowered the “denitrification” $\delta^{15}\text{N}$ signal (Thunell and Kepple, 2004). Lastly, enrichment of the sedimentary $\delta^{15}\text{N}$ values occurs during early burial, where oxygen exposure results in enhanced biological isotopic alteration (Robinson et al., 2012). In short, sedimentary $\delta^{15}\text{N}$ is shaped by many opposing processes, and assuming a one-to-one relationship with denitrification intensities and DO concentration clearly misses the complexity that shapes the CCS. Ladderanes hereby offer a more detailed picture of N-loss dynamics in the paleo-environment of the CCS. In the case of the ODP Site 1012 record, ladderane concentration trends challenge the conventional assumption that N-loss processes solely follow ocean circulation and ventilation patterns coupled to (inter)glacial cycling and instead show OM remineralization may also be an important driver of N loss.

Discrepancies between the ladderane and $\delta^{15}\text{N}$ record hereby necessitate careful consideration when applying N-isotope-based budgets to estimate past N cycling. More specifically, the occurrence of increased ladderane concentrations during glacial maxima may require a re-evaluation on the response of N-loss rates to glacial–interglacial cycling in the CCS. Furthermore, the occurrence of an additional N-loss pathway in the CCS (anammox), other than denitrification, may affect estimates of N_2O greenhouse gas production by denitrifiers and the degree of heterotrophy of the system, although the importance of this would require further investigation. Future research, investigating anammox biomarkers in other CCS records (preferably in a latitudinal gradient with this record) may offer further insights into N-loss dynamics across glacial–interglacial cycles.

6 Conclusions

Ladderane FAs detected in a ~ 500 kyr CCS sedimentary record at ODP Site 1012 reveal the past occurrence of anaerobic ammonium oxidizing (anammox) bacteria in the water column of the California Current system (CCS) over the last five glacial terminations. The index of ladderanes with five cyclobutane moieties (NL_5), which correlates with the in situ temperature at which ladderanes are synthesized, suggests that ladderanes were derived from the ESTNP OMZ water column. The CCS record shows a continuous presence of ladderane FAs over the last two interglacial–glacial transitions,

with maxima during (i) the Holocene, (ii) leading up to and during the LGM (early MIS 3 to mid-MIS 2), (iii) MIS 5b-c, and (iv) during the ice sheet maxima of the penultimate glacial (late MIS 6). Combining information on the presence of ladderanes with paleo-productivity proxies and the hydrographic features of the CCS suggests anammox abundance was driven by both OM remineralization and advection changes, which regulated nutrient and oxygen concentrations. In the record, a clear shift is seen in the relationship of SC ladderanes over their parent products, in which the relative abundance of SC ladderanes is significantly lower in Holocene than in pre-Holocene sediments. This may reflect a shift in oxygen exposure, which corresponds to previous studies showcasing a vertical expansion of the ENP OMZ over the Holocene. Clearly, the anammox contribution to N loss in the CCS, as shown in this study, requires a re-assessment of biogeochemical cycling in this system. Discrepancies between the ladderane and $\delta^{15}\text{N}$ record may imply that N loss was perhaps more intense during cold phases than previously assumed. Careful considerations must thus be taken when using N-isotope based budgets to estimate past N cycling in the CCS; sedimentary $\delta^{15}\text{N}$ is shaped by many opposing processes, and assuming a one-to-one relationship between N-loss intensities and OMZ variability clearly overlooks the complexity that shapes the CCS. Ladderanes hereby offer a more holistic picture of N-loss dynamics in the paleo-environment of the CCS.

Data availability. All data discussed in this paper are available in the Supplement. Data from the Supplement can be retrieved via <https://doi.org/10.25850/nioz/7b.b.sg> (van Kemenade, 2023).

Supplement. The supplement related to this article is available online at: <https://doi.org/10.5194/bg-21-1517-2024-supplement>.

Author contributions. ZE and ZRvK performed the laboratory work. ZRvK conducted the data analysis and writing of the manuscript. ZE created the age-model. ECH developed and optimized the UHPLC-HRMS method for the analysis of ladderane lipids. DR provided the supervision of the project. DR, ZE and ZRvK designed and conceptualized the project. JSSD provided critical support in data interpretation. All authors contributed to the writing of the manuscript.

Competing interests. The contact author has declared that none of the authors has any competing interests.

Disclaimer. Publisher’s note: Copernicus Publications remains neutral with regard to jurisdictional claims made in the text, published maps, institutional affiliations, or any other geographical representation in this paper. While Copernicus Publications makes ev-

ery effort to include appropriate place names, the final responsibility lies with the authors.

Special issue statement. This article is part of the special issue “Low-oxygen environments and deoxygenation in open and coastal marine waters”. It is not associated with a conference.

Acknowledgements. We thank the captain and crew in charge of Ocean Drilling Program Leg 167 for the collection of all sampled material used in this study. Denise Dorhout and Monique Verweij are also greatly appreciated for their support with the instrumental analysis. We also kindly thank Ronald van Bommel and Marcel van der Meer for their help in the isotope lab.

Financial support. This research has been supported by the Soehngen Institute of Anaerobic Microbiology (grant no. 024.002.002), awarded to Jaap Smede Sinninghe Damsté by the Dutch Ministry of Education, Culture and Science (OCW).

Review statement. This paper was edited by Sebastian Naeher and reviewed by two anonymous referees.

References

- Altabet, M. A. and Francois, R.: Sedimentary nitrogen isotopic ratio as a recorder for surface ocean nitrate utilization, *Global Biogeochem. Cy.*, 8, 103–116, <https://doi.org/10.1029/93GB03396>, 1994.
- Altabet, M. A., Pilskaln, C., Thunell, R., Pride, C., Sigman, D., Chavez, F., and Francois, R.: The nitrogen isotope biogeochemistry of sinking particles from the margin of the eastern North Pacific, *Deep-Sea Res. Pt. 1*, 46, 655–679, [https://doi.org/10.1016/S0967-0637\(98\)00084-3](https://doi.org/10.1016/S0967-0637(98)00084-3), 1999.
- Anderson, R. F., Sachs, J. P., Fleisher, M. Q., Allen, K. A., Yu, J., Koutavas, A., and Jaccard, S. L.: Deep-Sea Oxygen Depletion and Ocean Carbon Sequestration During the Last Ice Age, *Global Biogeochem. Cy.*, 33, 301–317, 2019.
- Babbin, A. R., Babbin, A. R., Keil, R. G., Devol, A. H., and Ward, B. B.: Oxygen Control Nitrogen Loss in the Ocean, *Science*, 344, 406–408, <https://doi.org/10.1126/science.1248364>, 2014.
- Bakun, A. and Nelson, C. S.: The seasonal cycle of wind-stress curl in subtropical eastern boundary current regions, *J. Phys. Oceanogr.*, 21, 1815–1834, [https://doi.org/10.1175/1520-0485\(1991\)021<1815:TSCOWS>2.0.CO;2](https://doi.org/10.1175/1520-0485(1991)021<1815:TSCOWS>2.0.CO;2), 1991.
- Bograd, S. J., Castro, C. G., di Lorenzo, E., Palacios, D. M., Bailey, H., Gilly, W., and Chavez, F. P.: Oxygen declines and the shoaling of the hypoxic boundary in the California Current, *Geophys. Res. Lett.*, 35, 1–6, <https://doi.org/10.1029/2008GL034185>, 2008.
- Bograd, S. J., Schroeder, I., Sarkar, N., Qiu, X., Sydeman, W. J., and Schwing, F. B.: Phenology of coastal upwelling in the California Current, *Geophys. Res. Lett.*, 36, 1–5, <https://doi.org/10.1029/2008GL035933>, 2009.
- Garcia, H. E., Boyer, T. P., Baranova, O. K., Locarnini, R. A., Mishonov, A. V., Grodsky, A., Paver, C. R., Weathers, K. W., Smolyar, I. V., Reagan, J. R., Seidov, D., and Zweng, M. M.: World Ocean Atlas 2018, NCEI [data set], <https://www.ncei.noaa.gov/data/oceans/woa/WOA18/DATA/> (last access: 4 December 2023), 2019.
- Brunner, B., Contreras, S., Lehmann, M. F., Matantseva, O., Rollog, M., and Kalvelage, T.: Nitrogen isotope effects induced by anammox bacteria, *P. Natl. Acad. Sci. USA*, 110, 18994–18999, <https://doi.org/10.1073/pnas.1310488110>, 2013.
- Canuel, E. A. and Martens, C. S.: Reactivity of recently deposited organic matter: near the sediment-water Degradation interface of lipid compounds, *Geochim. Cosmochim. Ac.*, 60, 1793–1806, 1996.
- Cartapanis, O., Tachikawa, K., and Bard, E.: Northeastern Pacific oxygen minimum zone variability over the past 70 kyr: Impact of biological production and oceanic ventilation, *Paleoceanogr. Paleoecol.*, 26, 1–17, <https://doi.org/10.1029/2011PA002126>, 2011.
- Castro, C. G., Chavez, F. P., and Collins, C. A.: Role of the California undercurrent in the export of denitrified waters from the eastern tropical North Pacific, *Global Biogeochem. Cy.*, 15, 819–830, <https://doi.org/10.1029/2000GB001324>, 2001.
- Chavez, F. P. and Messié, M.: A comparison of Eastern Boundary Upwelling Ecosystems, *Prog. Oceanogr.*, 83, 80–96, <https://doi.org/10.1016/j.pocean.2009.07.032>, 2009.
- Checkley, D. M. and Barth, J. A.: Patterns and processes in the California Current System, *Prog. Oceanogr.*, 83, 49–64, <https://doi.org/10.1016/j.pocean.2009.07.028>, 2009.
- Choumiline, K., Pérez-Cruz, L., Gray, A. B., Bates, S. M., and Lyons, T. W.: Scenarios of Deoxygenation of the Eastern Tropical North Pacific During the Past Millennium as a Window Into the Future of Oxygen Minimum Zones, *Front. Earth Sci.*, 7, 1–23, <https://doi.org/10.3389/feart.2019.00237>, 2019.
- Codispoti, L. A., Brandes, J. A., Christensen, J. P., Devol, A. H., Naqvi, S. W. A., Paerl, H. W., and Yoshinari, T.: The oceanic fixed nitrogen and nitrous oxide budgets: Moving targets as we enter the anthropocene?, *Sci. Mar.*, 65, 85–105, <https://doi.org/10.3989/scimar.2001.65s285>, 2001.
- Dalsgaard, T., Thamdrup, B., Farías, L., and Revsbech, N. P.: Anammox and denitrification in the oxygen minimum zone of the eastern South Pacific, *Limnol. Oceanogr.*, 57, 1331–1346, <https://doi.org/10.4319/lo.2012.57.5.1331>, 2012.
- Dorman, C. E. and Winanat, C. D.: Buoy observations of the atmosphere along the west coast of the United States, 1981–1990, *J. Geophys. Res.*, 100, 1981–1990, <https://doi.org/10.1029/95jc00964>, 1995.
- Fine, R. A., Maillet, K. A., Sullivan, K. F., and Willey, D.: Circulation and Ventilation flux of the Pacific Ocean, *J. Geophys. Res.-Ocean.*, 106, 22159–22178, <https://doi.org/10.1029/1999jc000184>, 2001.
- Frigstad, H., Andersen, T., Hessen, D. O., Naustvoll, L. J., Johnsen, T. M., and Bellerby, R. G. J.: Seasonal variation in marine C:N:P stoichiometry: Can the composition of seston explain stable Redfield ratios?, *Biogeosciences*, 8, 2917–2933, <https://doi.org/10.5194/bg-8-2917-2011>, 2011.
- Fu, W., Bardin, A., and Primeau, F.: Tracing ventilation source of tropical Pacific oxygen minimum zones with an adjoint global ocean transport model, *Deep-Sea Res. Pt. 1*, 139, 95–103, <https://doi.org/10.1016/j.dsr.2018.07.017>, 2018.

- Galán, A., Molina, V., Thamdrup, B., Woebken, D., Lavik, G., Kuypers, M. M. M., and Ulloa, O.: Anammox bacteria and the anaerobic oxidation of ammonium in the oxygen minimum zone off northern Chile, *Deep-Sea Res. Pt. 2*, 56, 1021–1031, <https://doi.org/10.1016/j.dsr2.2008.09.016>, 2009.
- Ganeshram, R. S., Pedersen, T. F., Calvert, S. E., McNeill, G. W., and Fontugne, M. R.: Glacial-interglacial variability in denitrification in the World's Oceans: Causes and consequences, *Paleoceanography*, 15, 361–367, 2000.
- Gruber, N.: The Dynamics of the Marine Nitrogen Cycle and its Influence on Atmospheric CO₂ Variations, in: *The Ocean Carbon Cycle and Climate*, edited by: Follows, M. and Oguz, T., Springer, Dordrecht, 97–148, <https://doi.org/10.1007/978-1-4020-2087-2>, 2004.
- Hamasaki, K., Shishikura, R., Suzuki, S., Shiozaki, T., Ogawa, H., Nakamura, T., and Suwa, Y.: Distribution and phylogeny of anaerobic ammonium-oxidizing (anammox) bacteria in the water column of the central Pacific Ocean, *Deep-Sea Res. Pt. 2*, 156, 60–67, <https://doi.org/10.1016/j.dsr2.2017.11.013>, 2018.
- Hamersley, M. R., Lavik, G., Woebken, D., Rattray, J. E., Lam, P., Hopmans, E. C., Sinninghe Damsté, J. S., Krüger, S., Graco, M., Gutiérrez, D., and Kuypers, M. M. M.: Anaerobic ammonium oxidation in the Peruvian oxygen minimum zone, *Limnol. Oceanogr.*, 52, 923–933, <https://doi.org/10.4319/lo.2007.52.3.0923>, 2007.
- Hendy, I. L. and Kennett, J. P.: Tropical forcing of North Pacific intermediate water distribution during Late Quaternary rapid climate change?, *Quaternary Sci. Rev.*, 22, 673–689, [https://doi.org/10.1016/S0277-3791\(02\)00186-5](https://doi.org/10.1016/S0277-3791(02)00186-5), 2003.
- Hendy, I. L. and Pedersen, T. F.: Oxygen minimum zone expansion in the Eastern Tropical North Pacific during deglaciation, *Geophys. Res. Lett.*, 33, 1–5, <https://doi.org/10.1029/2006GL025975>, 2006.
- Herbert, T. D., Schuffert, J. D., Andreasen, D., Heusser, L., Lyle, M., Mix, A., Ravelo, A. C., Stott, L. D., and Herguera, J. C.: Collapse of the California current during glacial maxima linked to climate change on land, *Science*, 293, 71–76, <https://doi.org/10.1126/science.1059209>, 2001.
- Herguera, J. C., Herbert, T., Kashgarian, M., and Charles, C.: Intermediate and deep water mass distribution in the Pacific during the Last Glacial Maximum inferred from oxygen and carbon stable isotopes, *Quaternary Sci. Rev.*, 29, 1228–1245, <https://doi.org/10.1016/j.quascirev.2010.02.009>, 2010.
- Hopmans, E. C., Kienhuis, M. V. V., Rattray, J. E., Jaeschke, A., Schouten, S., and Sinninghe Damsté, J. S.: Improved analysis of ladderane lipids in biomass and sediments using high-performance liquid chromatography/atmospheric pressure chemical ionization tandem mass spectrometry, *Rapid Commun. Mass Sp.*, 20, 2099–2103, 2006.
- Huyer, A.: Coastal upwelling in the California current system, *Prog. Oceanogr.*, 12, 259–284, [https://doi.org/10.1016/0079-6611\(83\)90010-1](https://doi.org/10.1016/0079-6611(83)90010-1), 1983.
- Jaeschke, A., Ziegler, M., Hopmans, E. C., Reichert, G. J., Lourens, L. J., and Schouten, S.: Molecular fossil evidence for anaerobic ammonium oxidation in the Arabian Sea over the last glacial cycle, *Paleoceanography*, 24, PA2202, <https://doi.org/10.1029/2008PA001712>, 2009.
- Kalvelage, T., Lavik, G., Lam, P., Contreras, S., Arteaga, L., Löscher, C. R., Oschlies, A., Paulmier, A., Stramma, L., and Kuypers, M. M. M.: Nitrogen cycling driven by organic matter export in the South Pacific oxygen minimum zone, *Nat. Geosci.*, 6, 228–234, <https://doi.org/10.1038/ngeo1739>, 2013.
- van Kemenade, Z. R., Villanueva, L., Hopmans, E. C., Kraal, P., Witte, H. J., Sinninghe Damsté, J. S., and Rush, D.: Bacteriohopanetetrol-*x*: Constraining its application as a lipid biomarker for marine anammox using the water column oxygen gradient of the Benguela upwelling system, *Biogeosciences*, 19, 201–221, <https://doi.org/10.5194/bg-19-201-2022>, 2022.
- Kemp, A. E. S., Langhorne, D. N., Fairchild, I. J., Schmitt, T. S., and Nisbet, E. G.: Evidence for abrupt climate changes in annually laminated marine sediments, *Philos. T. R. Soc. A*, 361, 1851–1870, <https://doi.org/10.1098/rsta.2003.1247>, 2003.
- Kienast, S. S., Calvert, S. E., and Pedersen, T. F.: Nitrogen isotope and productivity variations along the north-east Pacific margin over the last 120 kyr: Surface and subsurface paleoceanography, *Paleoceanography*, 17, 7-1–7-17, <https://doi.org/10.1029/2001PA000650>, 2002.
- Kobayashi, K., Makabe, A., Yano, M., Oshiki, M., Kindaichi, T., Casciotti, K. L., and Okabe, S.: Dual nitrogen and oxygen isotope fractionation during anaerobic ammonium oxidation by anammox bacteria, *ISME J.*, 13, 2426–2436, <https://doi.org/10.1038/s41396-019-0440-x>, 2019.
- Koeve, W. and Kähler, P.: Heterotrophic denitrification vs. autotrophic anammox-quantifying collateral effects on the oceanic carbon cycle, *Biogeosciences*, 7, 2327–2337, <https://doi.org/10.5194/bg-7-2327-2010>, 2010.
- Kuenen, J. G. and Robertson, L. A.: Ecology of Nitrification and Denitrification-Book.pdf, in: *The Nitrogen and Sulphur Cycles*, edited by: Cole, J. A. and Ferguson, S., Cambridge University Press, 162–218, ISBN: 0-521-35199-5, 1988.
- Kuypers, M. M. M., Silekers, A. O., Lavik, G., Schmid, M., Jørgensen, B. B., Kuenen, J. G., Sinninghe Damsté, J. S., Strous, M., and Jetten, M. S. M.: Anaerobic ammonium oxidation by anammox bacteria in the Black Sea, *Nature*, 422, 608–611, <https://doi.org/10.1038/nature01472>, 2003.
- Laffoley, D. and Baxter, J. M.: Ocean deoxygenation : everyone's problem. Summary for policy makers, IUCN, Gland, <https://doi.org/10.2305/iucn.ch.2019.14.en>, 2019.
- Lamb, A. L., Wilson, G. P., and Leng, M. J.: A review of coastal palaeoclimate and relative sea-level reconstructions using $\delta^{13}\text{C}$ and C/N ratios in organic material, *Earth Sci. Rev.*, 75, 29–57, <https://doi.org/10.1016/j.earscirev.2005.10.003>, 2006.
- Lembke-Jene, L., Tiedemann, R., Nürnberg, D., Gong, X., and Lohmann, G.: Rapid shift and millennial-scale variations in Holocene North Pacific intermediate water ventilation, *P. Natl. Acad. Sci. USA*, 115, 5365–5370, <https://doi.org/10.1073/pnas.1714754115>, 2018.
- Liu, Z., Altabet, M. A., and Herbert, T. D.: Glacial-interglacial modulation of eastern tropical North Pacific denitrification over the last 1.8-Myr, *Geophys. Res. Lett.*, 32, 1–4, <https://doi.org/10.1029/2005GL024439>, 2005.
- Lu, Z., Hoogakker, B. A. A., Hillenbrand, C. D., Zhou, X., Thomas, E., Gutchess, K. M., Lu, W., Jones, L., and Rickaby, R. E. M.: Oxygen depletion recorded in upper waters of the glacial Southern Ocean, *Nat. Commun.*, 7, 11146, <https://doi.org/10.1038/ncomms11146>, 2016.
- Lyle, M., Koizumi, I., Richter, C., Fox, P. J., Balda, J., and Francis, T. J. G.: Proceedings of the Ocean

- Drilling Program, *Clin. Orthop. Relat. R.*, 465, 106–111, <https://doi.org/10.1097/BLO.0b013e3181576080>, 1997.
- Mercer, J. L., Zhao, M., and Colman, S. M.: Seasonal variations of alkenones and UK37 in the Chesapeake Bay water column, *Estuar. Coast. Shelf Sci.*, 63, 675–682, <https://doi.org/10.1016/j.ecss.2005.01.011>, 2005.
- Matsumoto, K., Tanioka, T., and Rickaby, R.: Linkages between dynamic phytoplankton C:N:P and the ocean carbon cycle under climate change, *Oceanography*, 33, 44–52, <https://doi.org/10.5670/oceanog.2020.203>, 2020.
- Matul, A., Abelmann, A., Khusid, T., Chekhovskaya, M., Kaiser, A., Nürnberg, D., and Tiedemann, R.: Late Quaternary changes of the oxygen conditions in the bottom and intermediate waters on the western Kamchatka continental slope, the Sea of Okhotsk, *Deep-Sea Res. Pt. 2*, 125/126, 184–190, <https://doi.org/10.1016/j.dsr2.2013.03.023>, 2016.
- Nicholson, S. E. and Flohn, H.: African climatic changes in late Pleistocene and Holocene and the general atmospheric circulation, *Clim. Change*, 2, 313–348, <https://doi.org/10.1007/BF00137203>, 1980.
- Ortiz, J., Mix, A., Hostetler, S., and Kashgarian, M.: The California Current of the Last Glacial Maximum: Reconstruction at 42° N based on multiple proxies, *Paleoceanography*, 12, 191–205, <https://doi.org/10.1029/96PA03165>, 1997.
- Paulmier, A. and Ruiz-Pino, D.: Oxygen minimum zones (OMZs) in the modern ocean, *Prog. Oceanogr.*, 80, 113–128, <https://doi.org/10.1016/j.pcean.2008.08.001>, 2009.
- Peng, X., Fuchsman, C. A., Jayakumar, A., Oleynik, S., Martens-Habbema, W., Devol, A. H., and Ward, B. B.: Ammonia and nitrite oxidation in the Eastern tropical North Pacific, *Global Biogeochem. Cy.*, 29, 2034–2049, <https://doi.org/10.1002/2015GB005278>, 2015.
- Peters, B., Horak, R., Devol, A., Fuchsman, C., Forbes, M., Mordy, C. W., and Casciotti, K. L.: Estimating fixed nitrogen loss and associated isotope effects using concentration and isotope measurements of NO_3^- , NO_2^- , and N_2 from the Eastern Tropical South Pacific oxygen deficient zone, *Deep-Sea Res. Pt. 2*, 156, 121–136, <https://doi.org/10.1016/j.dsr2.2018.02.011>, 2018.
- Pierce, S. D., Barth, J. A., Kipp Shearman, R., and Erofeev, A. Y.: Declining oxygen in the northeast Pacific, *J. Phys. Oceanogr.*, 42, 495–501, <https://doi.org/10.1175/JPO-D-11-0170.1>, 2012.
- Rattray, J. E., Van De Vossenberg, J., Hopmans, E. C., Kartal, B., Van Niftrik, L., Rijpstra, W. I. C., Strous, M., Jetten, M. S. M., Schouten, S., and Damsté, J. S. S.: Ladderane lipid distribution in four genera of anammox bacteria, *Arch. Microbiol.*, 190, 51–66, <https://doi.org/10.1007/s00203-008-0364-8>, 2008.
- Rattray, J. E., Van Vossenberg, J. De, Jaeschke, A., Hopmans, E. C., Wakeham, S. G., Lavik, G., Kuypers, M. M. M., Strous, M., Jetten, M. S. M., Schouten, S., and Sinninghe Damsté, J. S.: Impact of temperature on ladderane lipid distribution in anammox bacteria, *Appl. Environ. Microbiol.*, 76, 1596–1603, <https://doi.org/10.1128/AEM.01796-09>, 2010.
- Redfield, A. C., Ketchum, B. H., and Richards, F. A.: The influence of organisms on the composition of sea water, in: *The sea*, Vol. 2, edited by: Hill, M. N., Wiley Interscience, New York, 26–77, 1963.
- Reid, J. L.: On the total geostrophic circulation of the Pacific ocean: flow patterns, tracers, and transports, *Prog. Oceanogr.*, 39, 263–352, 1997.
- Reid, J. L. and Mantyla, A. W.: On the Mid-Depth Circulation of the North Pacific Ocean, *J. Phys. Oceanogr.*, 8, 946–951, [https://doi.org/10.1175/1520-0485\(1978\)008<0946:otmdco>2.0.co;2](https://doi.org/10.1175/1520-0485(1978)008<0946:otmdco>2.0.co;2), 1978.
- Robinson, R. S., Kienast, M., Albuquerque, A. L., Altabet, M., Contreras, S., Holz, R. D. P., Dubois, N., Francois, R., Galbraith, E., Hsu, T., Ivanochko, T., Jaccard, S., Kao, S., Kiefer, T., Kienast, S., Lehmann, M., Martinez, P., Mccarthy, M., Möbius, J., Pedersen, T., Quan, T. M., Ryabenko, E., Schmittner, A., Schneider, R., and Schneider-mor, A.: A review of nitrogen isotopic alteration in marine sediments, *Paleoceanography*, 27, PA4203, <https://doi.org/10.1029/2012PA002321>, 2012.
- Rush, D. and Sinninghe Damsté, J. S.: Lipids as paleomarkers to constrain the marine nitrogen cycle, *Environ. Microbiol.*, 19, 2119–2132, <https://doi.org/10.1111/1462-2920.13682>, 2017.
- Rush, D., Jaeschke, A., Hopmans, E. C., Geenevasen, J. A. J., Schouten, S., and Damsté, J. S. S.: Short chain ladderanes: Oxic biodegradation products of anammox lipids, *Geochim. Cosmochim. Ac.*, 75, 1662–1671, <https://doi.org/10.1016/j.gca.2011.01.013>, 2011.
- Rush, D., Wakeham, S. G., Hopmans, E. C., Schouten, S., and Sinninghe Damsté, J. S.: Biomarker evidence for anammox in the oxygen minimum zone of the Eastern Tropical North Pacific, *Org. Geochem.*, 53, 80–87, <https://doi.org/10.1016/j.orggeochem.2012.02.005>, 2012a.
- Rush, D., Hopmans, E. C., Wakeham, S. G., Schouten, S., and Sinninghe Damsté, J. S.: Occurrence and distribution of ladderane oxidation products in different oceanic regimes, *Biogeosciences*, 9, 2407–2418, <https://doi.org/10.5194/bg-9-2407-2012>, 2012b.
- Rush, D., Hopmans, E. C., Wakeham, S. G., Schouten, S., and Sinninghe Damsté, J. S.: Occurrence and distribution of ladderane oxidation products in different oceanic regimes, *Biogeosciences*, 9, 2407–2418, <https://doi.org/10.5194/bg-9-2407-2012>, 2012c.
- Rush, D., Talbot, H. M., Van Der Meer, M. T. J., Hopmans, E. C., Douglas, B., and Damsté, J. S. S.: Biomarker evidence for the occurrence of anaerobic ammonium oxidation in the eastern Mediterranean Sea during Quaternary and Pliocene sapropel formation, *Biogeosciences*, 16, 2467–2479, <https://doi.org/10.5194/bg-16-2467-2019>, 2019.
- Ryabenko, E.: Stable Isotope Methods for the Study of the Nitrogen Cycle, in: *Topics in Oceanography*, edited by: Zambianchi, E., 49–88, <https://doi.org/10.5772/56105>, 2013.
- Sahu, S., Allen, S. E., Saldías, G. S., Klymak, J. M., and Zhai, L.: Spatial and Temporal Origins of the La Perouse Low Oxygen Pool: A Combined Lagrangian Statistical Approach, *J. Geophys. Res.-Ocean.*, 127, 1–20, <https://doi.org/10.1029/2021JC018135>, 2022.
- Schneider, B., Schlitzer, R., Fischer, G., and Nöthig, E. M.: Depth-dependent elemental compositions of particulate organic matter (POM) in the ocean, *Global Biogeochem. Cy.*, 17, 1032, <https://doi.org/10.1029/2002gb001871>, 2003.
- Sigman, D. M. and Fripiat, F.: Nitrogen isotopes in the ocean, in: *Encyclopedia of Ocean Sciences*, edited by: Kirk Cochran, J., Bokuniewicz, H. J., and Yager, P. L., Elsevier, 263–278, <https://doi.org/10.1016/B978-0-12-409548-9.11605-7>, 2019.
- Sinninghe Damsté, J. S., Strous, M., Rijpstra, W. I. C., Hopmans, E. C., Geenevasen, J. A. J., Van Duin, A. C. T., Van Niftrik, L. A., and Jetten, M. S. M.: Linearly concatenated cyclobutane

- lipids form a dense bacterial membrane, *Nature*, 419, 708–712, <https://doi.org/10.1038/nature01067>, 2002.
- Smith, K. L., Messié, M., Connolly, T. P., and Huffard, C. L.: Decadal Time-Series Depletion of Dissolved Oxygen at Abyssal Depths in the Northeast Pacific, *Geophys. Res. Lett.*, 49, e2022GL101018, <https://doi.org/10.1029/2022GL101018>, 2022.
- Sollai, M., Hopmans, E. C., Schouten, S., Keil, R. G., and Sinninghe Damsté, J. S.: Intact polar lipids of Thaumarchaeota and anammox bacteria as indicators of N cycling in the eastern tropical North Pacific oxygen-deficient zone, *Biogeosciences*, 12, 4725–4737, <https://doi.org/10.5194/bg-12-4725-2015>, 2015.
- Sonnerup, R. E., Quay, P. D., and Bullister, J. L.: Thermocline ventilation and oxygen utilization rates in the subtropical North Pacific based on CFC distributions during WOCE, *Deep-Sea Res. Pt. 1*, 46, 777–805, [https://doi.org/10.1016/S0967-0637\(98\)00092-2](https://doi.org/10.1016/S0967-0637(98)00092-2), 1999.
- Stramma, L., Johnson, G. C., Firing, E., and Schmidtko, S.: Eastern Pacific oxygen minimum zones: Supply paths and multidecadal changes, *J. Geophys. Res.-Ocean.*, 115, 1–12, <https://doi.org/10.1029/2009JC005976>, 2010.
- Sverdrup, H. U., Johnson, M. W., and Fleming, R. H.: *The Oceans, Their Physics, Chemistry, and General Biology*. Prentice-Hall, New York, <http://ark.cdlib.org/ark:/13030/kt167nb66r>, 1942.
- Tesdal, J. E., Galbraith, E. D., and Kienast, M.: Nitrogen isotopes in bulk marine sediment: Linking seafloor observations with subseafloor records, *Biogeosciences*, 10, 101–118, <https://doi.org/10.5194/bg-10-101-2013>, 2013.
- Thamdrup, B., Dalsgaard, T., Jensen, M. M., Ulloa, O., Farías, L., and Escribano, R.: Anaerobic ammonium oxidation in the oxygen-deficient waters off northern Chile, *Limnol. Oceanogr.*, 51, 2145–2156, <https://doi.org/10.4319/lo.2006.51.5.2145>, 2006.
- Thomson, R. E. and Krassovski, M. V.: Poleward reach of the California Undercurrent extension, *J. Geophys. Res.-Ocean.*, 115, C09027, <https://doi.org/10.1029/2010JC006280>, 2010.
- Thunell, R. C. and Kepple, A. B.: Glacial-Holocene $\delta^{15}\text{N}$ record from the Gulf of Tehuantepec, Mexico: Implications for denitrification in the eastern equatorial Pacific and changes in atmospheric N_2O , *Global Biogeochem. Cy.*, 18, GB1001, <https://doi.org/10.1029/2002GB002028>, 2004.
- Vallero, D. A.: Air pollution biogeochemistry, in: *Air Pollution Calculations*, edited by: Vallero, D. A., Elsevier, 175–206, <https://doi.org/10.1016/b978-0-12-814934-8.00008-9>, 2019.
- van de Graaf, A. A., Mulder, A., de Bruijn, P., Jetten, M. S. M., Robertson, L. A., and Kuenen, J. G.: Anaerobic oxidation of ammonium is a biologically mediated process, *Appl. Environ. Microbiol.*, 61, 1246–1251, <https://doi.org/10.1128/aem.61.4.1246-1251.1995>, 1995.
- van de Graaf, A. A., de Bruijn, P., Robertson, L. A., Jetten, M. S. M., and Kuenen, J. G.: Metabolic pathway of anaerobic ammonium oxidation on the basis of ^{15}N studies in a fluidized bed reactor, *Microbiology*, 143, 2415–2421, <https://doi.org/10.1099/00221287-143-7-2415>, 1997.
- van Kemenade, Z.: Loss of nitrogen via anaerobic ammonium oxidation (anammox) in the California current system during the late Quaternary, NIOZ [data set], <https://doi.org/10.25850/nioz/7b.b.sg>, 2023.
- van Kemenade, Z. R., Cutmore, A., Hennekam, R., Hopmans, E. C., van der Meer, M. T. J., Mojtahid, M., Jorissen, F. J., Bale, N. J., Reichart, G. J., Sinninghe Damsté, J. S., and Rush, D.: Marine nitrogen cycling dynamics under altering redox conditions: Insights from deposition of sapropels S1 and the ambiguous S2 in the Eastern Mediterranean Sea, *Geochim. Cosmochim. Ac.*, 354, 197–210, <https://doi.org/10.1016/j.gca.2023.06.018>, 2023.
- Verardo, D. J. and McIntyre, A.: Production and destruction: Control of biogenous sedimentation in the tropical Atlantic 0–300,000 years B.P., *Paleoceanography*, 9, 63–86, <https://doi.org/10.1029/93PA02901>, 1994.
- Vossenberg, J. Van De, Rattray, J. E., Geerts, W., Kartal, B., Niftrik, L. Van, Donselaar, E. G. Van, Damsté, J. S. S., Strous, M., and Jetten, M. S. M.: Enrichment and characterization of marine anammox bacteria associated with global nitrogen gas production, *Environ. Microbiol.*, 10, 3120–3129, <https://doi.org/10.1111/j.1462-2920.2008.01643.x>, 2008.
- Wang, Y., Hendy, I. L., and Zhu, J.: Expansion of the Southern California oxygen minimum zone during the early-to mid-Holocene due to reduced ventilation of the Northeast Pacific, *Quaternary Sci. Rev.*, 238, 106326, <https://doi.org/10.1016/j.quascirev.2020.106326>, 2020.
- Ward, B. B.: How nitrogen is lost, *Science*, 341, 352–353, <https://doi.org/10.1126/science.1240314>, 2013.
- White, M. E., Rafter, P. A., Stephens, B. M., Wankel, S. D., and Aluwihare, L. I.: Recent Increases in Water Column Denitrification in the Seasonally Suboxic Bottom Waters of the Santa Barbara Basin, *Geophys. Res. Lett.*, 46, 6786–6795, <https://doi.org/10.1029/2019GL082075>, 2019.
- Whitney, F. A., Freeland, H. J., and Robert, M.: Persistently declining oxygen levels in the interior waters of the eastern subarctic Pacific, *Prog. Oceanogr.*, 75, 179–199, <https://doi.org/10.1016/j.pocean.2007.08.007>, 2007.
- Worne, S., Kender, S., Swann, G. E. A., Leng, M. J., and Ravelo, A. C.: Coupled climate and subarctic Pacific nutrient upwelling over the last 850,000 years, *Earth Planet Sc. Lett.*, 522, 87–97, <https://doi.org/10.1016/j.epsl.2019.06.028>, 2019.
- Yamamoto, M., Yamamoto, M., and Tanaka, Y.: The California current system during the last 136,000 years: response of the North Pacific High to precessional forcing, *Quaternary Sci. Rev.*, 26, 405–414, <https://doi.org/10.1016/j.quascirev.2006.07.014>, 2007.
- Zhou, Y., Gong, H., and Zhou, F.: Responses of Horizontally Expanding Oceanic Oxygen Minimum Zones to Climate Change Based on Observations, *Geophys. Res. Lett.*, 49, 1–11, <https://doi.org/10.1029/2022GL097724>, 2022.
- Zonneveld, K. A. F., Versteegh, G. J. M., Kasten, S., Eglinton, T. I., Emeis, K.-C., Huguet, C., Koch, B. P., de Lange, G. J., de Leeuw, J. W., Middelburg, J. J., Mollenhauer, G., Prahl, F. G., Rethemeyer, J., and Wakeham, S. G.: Selective preservation of organic matter in marine environments; processes and impact on the sedimentary record, *Biogeosciences*, 7, 483–511, <https://doi.org/10.5194/bg-7-483-2010>, 2010.